

INTERNATIONAL SOCIETY FOR SOIL MECHANICS AND GEOTECHNICAL ENGINEERING



This paper was downloaded from the Online Library of the International Society for Soil Mechanics and Geotechnical Engineering (ISSMGE). The library is available here:

<https://www.issmge.org/publications/online-library>

This is an open-access database that archives thousands of papers published under the Auspices of the ISSMGE and maintained by the Innovation and Development Committee of ISSMGE.

Consolidation behavior of Shanghai clay under cyclic loading

Comportement de consolidation de l'argile de Shanghai sous chargement cyclique

X.Y.Gu & D.N.Xu – *Institute of Mechanics, Chinese Academy of Sciences, People's Republic of China*

ABSTRACT: In this paper the experiments of the primary and secondary consolidation behavior of Shanghai clay under the cyclic loading with period of several minutes, simulating the characteristics of yearly periodical fluctuation of the water level, are conducted. The factors such as the loading wave shape, cyclic loading parameters, loading order, consolidation state, existence of secondary consolidation before cyclic loading, are investigated. The superposition theorem between the accumulated deformation and secondary consolidation is verified. The pore pressure development is also measured in some cases. The test results provide the model and the nonlinear soil parameters for the computation of land subsidence, and also serves the basis of measures for slowing down the subsidence rate.

RESUME: Dans ce papier les résultats expérimentaux sur les consolidations primaires et secondaires sur l'argile de Shanghai, sous le cycle de chargement avec une période de minutes réelles, sont conduites pour simuler les caractéristiques d'une période annuelle de fluctuation du niveau de l'eau. Les facteurs telles que le chargement de la forme de l'onde, le cycle de chargement des paramètres, l'ordre de chargement, l'état de consolidation, l'existence de consolidation secondaire avant le cycle chargement, ont été étudiés. Le théorème de superposition entre la déformation accumulée et la consolidation secondaire est vérifié. Le développement de la pression du pore est aussi mesuré dans quelques cas. Les tests résultats produisent le modèle et les paramètres terriens non linéaire pour le calcul de l'affaissement du terrain et servent aussi pour la mesure basic de la descente lente du taux d'affaissement.

1 INTRODUCTION

The primary consolidation theory has been applied rather successfully for computation of land subsidence due to water withdrawal in Shanghai for quite a number of years (Tsien & Gu 1981). However, since 1981 some divergency appears between the computation results and the observed data, especially for the areas where the clay layers above the aquifer (Figure 1) possess the rheological properties. Thus the effect of the secondary consolidation should also be considered in computation (Gu et al 1991).

The groundwater level of the aquifer, which causes the land subsidence in Shanghai, has the characteristics of yearly periodical fluctuation (Figure 2). According to the water level change, the stress-strain diagram can be drawn as shown in Figure 3. In order to verify the computation model and obtain the soil parameters, the experiments for studying the primary and secondary consolidation behavior of Shanghai clay under the cyclic loading simulating the above characteristics, are conducted.

2 TEST PROCEDURE

Because of the rationality of one-dimensional problem of land subsidence in Shanghai, the experiments are conducted in oedometers. Before applying the cyclic loading samples are subjected to initial pressure P_0 , and after the cyclic stage the secondary consolidation is investigated for two weeks. The laboratory temperature is maintained constant with errors $\pm 0.5^\circ\text{C}$.

In order to obtain the soil parameters which reflect the real situation, the following factors are investigated:

1. Shape of loading wave

The sinusoidal wave shape is closer to the actual water level fluctuation. However, the rectangular wave shape can be operated more easily and has the advantage of obtaining the coefficients of consolidation for compression and rebound



Figure 1. Soil profile

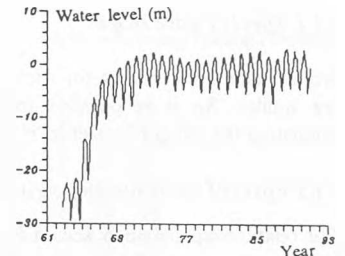


Figure 2. Water level change

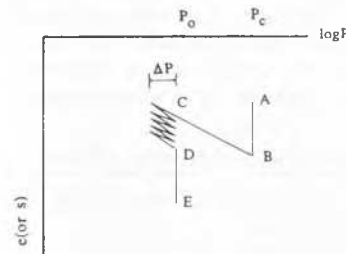


Figure 3. Stress-strain diagram due to water pumpage

conditions. So tests with these two wave shapes are compared.

2. Parameters of cyclic loading

The increment ΔP , period T of cyclic loading, and number of cycles N are involved herein. ΔP is determined by the actual water level change. The order of T is from one to several minutes.

3. Loading order

Usually cyclic tests are conducted under the loading-unloading pattern. However, from Figure 3, the unloading-loading pattern seems more suitable. Therefore, tests with both two patterns are investigated.

4. Overconsolidation state

Since the previous water level has been lower than the current one, the lower part of the second compressible layer, locating

near the aquifer, becomes slightly overconsolidated, OCR of which equals 1.5. The difference between the consolidation behavior of normally consolidated and overconsolidated soil under cyclic loading is investigated.

5. Effect of secondary consolidation before cyclic loading

In actual condition, it is unknown whether the secondary consolidation has taken place before cyclic loading. Therefore, two series of tests are compared. Series A: Before applying the cyclic loading consolidate the sample under initial pressure P_0 for 24 hours. Series B: No sooner the primary consolidation under P_0 has completed, than the cyclic loading is applied, and after cyclic loading the secondary consolidation is observed.

6. Relationship between accumulated deformation under cyclic loading and secondary consolidation

Take three samples for which primary consolidation under P_0 has completed. To the first one apply static pressure to $2P_0$ and observe secondary consolidation. To the second one apply cyclic loading and obtain the accumulated deformation. To the last one apply both static pressure to $2P_0$ and cyclic loading, then observe secondary consolidation. From the test results find out if the deformation of the third sample equals the sum of the first two's.

7. Pore pressure development

For distinction of primary and secondary consolidation the pore pressure is measured in some samples.

3 TEST RESULTS

3.1 Accumulated deformation caused by cyclic loading S_c

3.1.1 Effect of wave shape

From Table 1 the results for rectangular and sinusoidal wave are similar. So it is possible to use rectangular wave for simulating the effect of water level change.

3.1.2 Effect of cyclic loading parameters

The relationship between accumulated deformation and cyclic loading increment for five samples from the same layer is shown in Figure 4. S_c increases with the increase of ΔP . It means different cyclic loading increments reflecting the real condition should be applied to samples from different layers. For the first layer, very small increment brings about very small deformation, sometimes even no deformation is observed. While for the second compressible layer, ΔP is relatively large,

Table 1. Accumulated deformation S_c under different wave shapes

| Sample No. | Wave shape | Accumulated deformation(mm) |
|------------|-------------|-----------------------------|
| 28-3 | Sinusoidal | 0.048 |
| 28-4 | Rectangular | 0.049 |
| 18-5 | Sinusoidal | 0.004 |
| 18-2 | Rectangular | 0.002 |
| 15-2 | Sinusoidal | 0.130 |
| 15-4 | Rectangular | 0.147 |

Table 2. Accumulated deformation for different periods

| Sample No. | Period (min) | Number of cycles | Accumulated deformation (mm) |
|------------|--------------|------------------|------------------------------|
| 28-2 | 4 | 20 | 0.032 |
| 28-5 | 60 | 20 | 0.085 |
| 7-2 | 1 | 20 | 0.011 |
| 7-1 | 4 | 20 | 0.024 |
| 36-1 | 1 | 20 | 0.0025 |
| 36-3 | 4 | 20 | 0.011 |

and S_c is obvious. It implies the periodical fluctuation of water level has significant effect on the II compressible layer, but not on the I layer.

The figures in Table 2 shows that accumulated deformation increases with the increase of period. So T for different clay layer is decided from the following formula:

$$T = T_r H^2 / H_f^2 \quad (1)$$

where H -thickness of the drainage path, subscript f indicates the field condition.

Figure 5 is a typical deformation - cycle number curve. The accumulated deformation increases with the increase of cycle number N , but its increment has the descending tendency. The accumulated deformation is related to the difference of volume compression coefficients under loading and unloading conditions (m_{vc} - m_{vs}). The changes of m_{vc} and m_{vs} with N are shown in Figure 6. m_{vs} basically keeps constant. The relationship between m_{vc} and N depends on loading order, as shown below.

The changes of the consolidation coefficients C_{vc} and C_{vs} with N are shown in Figure 7. For first several cycles, $C_{vc} < C_{vs}$, but afterwards C_v stabilizes, i.e. $C_{vc} = C_{vs}$.

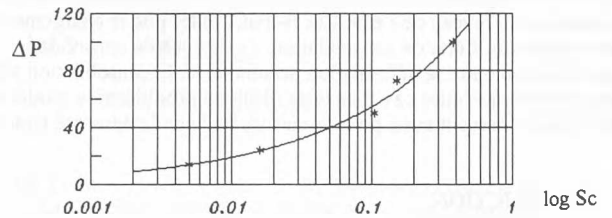


Figure 4. Accumulated deformation- cyclic loading increment curve

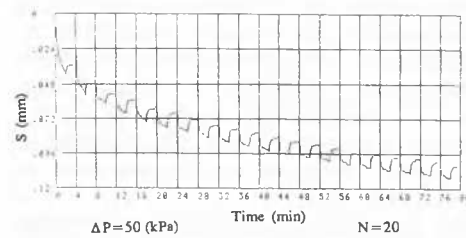


Figure 5. Accumulated deformation S - cycle number N curve

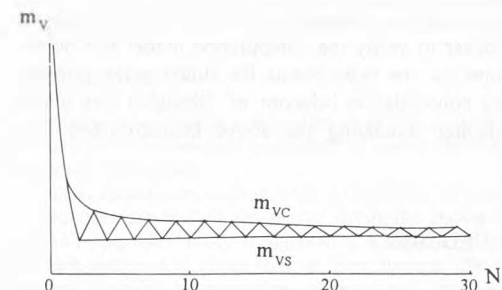


Figure 6. Change of volume compression coefficients with cycle number

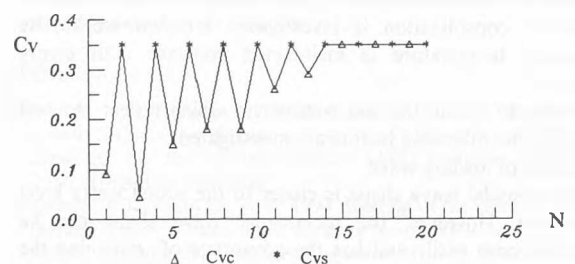


Figure 7. Change of consolidation coefficients with cycle number

3.1.3 Effect of loading order

The amount of accumulated deformation for the loading-unloading pattern is much larger than the one for the unloading-loading pattern under the same cyclic loading parameters. Figure 5 is the test result under loading-unloading condition, and Figure 8 for unloading-loading condition. The S-N relationship under loading-unloading pattern can be fitted by the exponential function:

$$\sum_{i=1}^N (m_{vc_i} - m_{vs_i}) = BN^{\alpha} \quad (2)$$

Since m_{vs} is a constant, the following formula can be obtained:

$$m_{vc} = B[N^{\alpha} - (N-1)^{\alpha}] + m_{vs} \quad (3)$$

When $N > 10$, the fitted results are somehow larger than the experimental data, so then m_{vc} are taken as different constants under different segments of N .

Under unloading-loading pattern, m_{vc} - N relationship has linear character for different segments of N . The curvilinear character can be observed only during first two cycles. So m_{vc} for unloading-loading pattern is represented by several constants.

For unloading-loading pattern, the stabilized C_v is much larger than that for the loading-unloading pattern, see Table 3.

Table 3. Stabilized consolidation coefficient under different loading patterns

| Sample No. | Loading order | Consolidation coefficient ($10 \text{ m}^2 / \text{s}$) |
|------------|---------------|---|
| 22-2 | L-U | 23 |
| 22-5 | U-L | 73 |
| 36-2 | L-U | 161 |
| 36-3 | U-L | 531 |

L-U: loading-unloading U-L: unloading-loading

3.1.4 Effect of overconsolidation state

The test result for the overconsolidation sample under unloading-loading condition is shown in Figure 9. The sample rebounds under cyclic loading, but the rebounding amount is quite small, and it stabilizes soon.

3.2 Secondary consolidation S_{α}

3.2.1 Secondary consolidation after cyclic loading

The whole consolidation curve for the unloading-loading condition is shown in Figure 10. The secondary consolidation coefficient doesn't change after the cyclic loading. For the loading-unloading condition, the whole consolidation curve is shown in Figure 11. The accumulated deformation S_c is much larger than the one for unloading-loading condition, C_{α} after cyclic loading is smaller than that before cyclic loading, and then increases gradually until it becomes the same value as that before cyclic loading. When S_c is even larger, the increasing tendency of C_{α} will be slower, it does not reach the value of C_{α} before cyclic loading within two weeks. Therefore, the change of C_{α} after cyclic loading depends on the loading order as well as the accumulated deformation S_c . When S_c is small, for both two loading patterns C_{α} doesn't change. When S_c is quite large for the loading-unloading pattern, C_{α} after cyclic loading is restrained for some time.

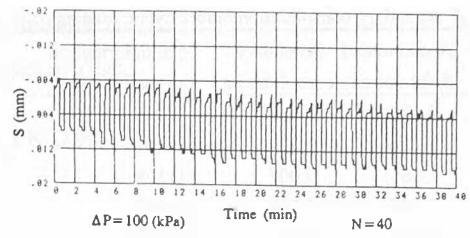


Figure 8. S - N curve under unloading-loading condition

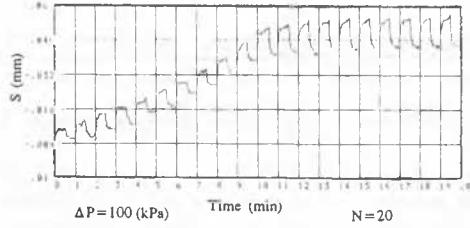


Figure 9. S - N curve of overconsolidated sample

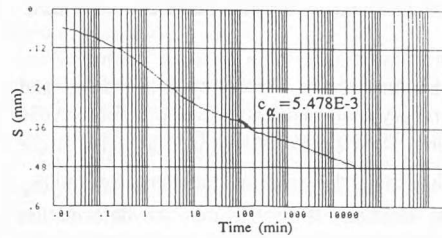


Figure 10. Whole consolidation curve for unloading-loading condition

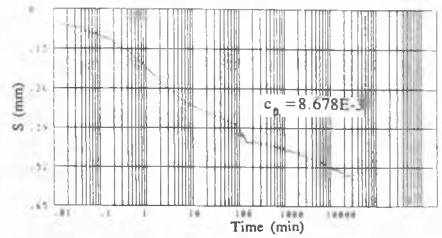


Figure 11. Whole consolidation curve for loading-unloading condition

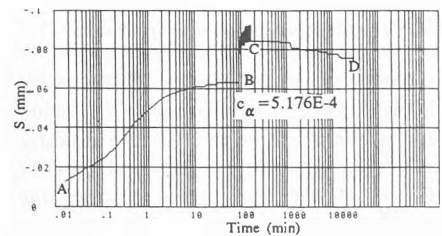


Figure 12. Whole consolidation curve for overconsolidated sample

For investigating the effect of overconsolidation state, apply the cyclic loading after unloading the sample from P_1 to P_0 , and then observe the secondary consolidation. The whole consolidation curve of the overconsolidated sample is obtained as shown in Figure 12. CD is the secondary consolidation part. Compare to the normally consolidated sample, C_{α} for the sample of $OCR=1.5$ reduces for about three times.

3.2.2 Effect of secondary consolidation before cyclic loading

S_c and S_{α} are obtained for two series of tests. Series A:

Table 4. Effect of secondary consolidation before cyclic loading

| Sample No. | Kind of test | Accumulated deformation | Secondary consolidation | Total deformation during 24 hours |
|------------|--------------|-------------------------|-------------------------|-----------------------------------|
| 8-3 | B | 0.077 | 0.029 | 0.106 |
| 8-4 | A | 0.026 | 0.074 | 0.100 |
| 22-2 | B | 0.161 | 0.007 | 0.168 |
| 22-3 | A | 0.107 | 0.060 | 0.167 |
| 36-3 | B | 0.016 | 0.043 | 0.059 |
| 36-4 | A | 0.004 | 0.054 | 0.058 |

Table 5. Verification of superposition theorem

| Sample No. | Primary consolidation S_0 (mm) | Loading increment | Deformation S (mm) | S/S_0 |
|------------|----------------------------------|--------------------|----------------------|---------|
| 18-1 | 0.599 | P_0 | 0.99 | 1.653 |
| 18-2 | 0.527 | $\pm\Delta P$ | 0.013 | 0.025 |
| 18-3 | 0.495 | $P_0 \pm \Delta P$ | 0.86 | 1.737 |
| 29-1 | 0.379 | P_0 | 0.484 | 1.277 |
| 29-2 | 0.420 | $\pm\Delta P$ | 0.048 | 0.114 |
| 29-3 | 0.357 | $P_0 \pm \Delta P$ | 0.493 | 1.381 |

Secondary consolidation occurs before cyclic loading, and series B: only primary consolidation occurs before cyclic loading. S_a for series A is smaller than that for series B (see Table 4). While the total deformation, including S_c and S_a , during 24 hours is identical. It implies that the deformation caused by cyclic loading and the secondary consolidation are mutually compensated.

3.2.3 Verification of superposition theorem

The results of the test groups with three parallel samples are shown in Table 5. In order to exclude the effect of sample differences, the amounts of deformation are divided by S_0 , the primary consolidation of this sample under P_0 . The figures in Table 5 indicate, deformation under both static pressure increment and cyclic loading (S/S_0), equals the sum of that for static pressure increment (S/S_0)₁ and for cyclic loading (S/S_0)₂. Thus the superposition theorem is verified. It means that S_c and S_a are uncoupled.

3.2.4 Relationship between pore pressure and deformation

Pore pressure-deformation curves under static and cyclic loading are shown in Figures 13 and 14 respectively. In Figure 13 the linear part during primary consolidation stage indicates the pore pressure and deformation are one-one correspondent, and the divergent part at the final stage indicates the development of secondary consolidation, i.e. the transition stage of primary and secondary consolidation. In the transition stage the amount of secondary consolidation is a small value compared to primary consolidation. Therefore, from the engineering view, considering secondary consolidation only after pore pressure dissipation will not bring large errors. However, strictly speaking, the occurrence of primary and secondary consolidation should not be considered separately. The average curve under cyclic loading (Figure 14) is basically a straight line until pore pressure dissipates to 6 kPa. This kind of relationship is similar to the one under static loading.

Application of the above test results is shown in the paper of Gu et al (1995). The computing model considering the secondary consolidation and the nonlinear parameters are obtained. The agreement between the computation results and observed data is good. Test results of overconsolidated samples

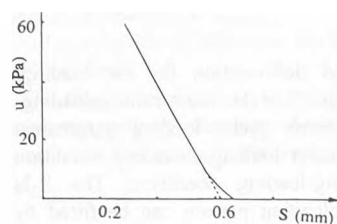


Figure 13. Pore pressure-deformation curve for static loading

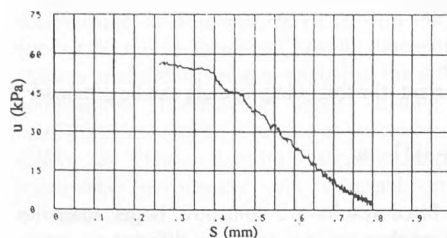


Figure 14. Pore pressure-deformation curve for cyclic loading

also provide the basis of measures for slowing down the subsidence rate.

4 CONCLUSION

In the study of consolidation behavior under cyclic loading simulating the characteristics of the water level change in Shanghai, vast amount of experiments, considering different factors, so as loading wave shape, cyclic loading parameters, loading order, consolidation state, mutual compensation between accumulated deformation and secondary consolidation, pore pressure development etc., have been conducted. The test results provide the model considering the secondary consolidation and soil parameters for the computation of land subsidence, as well as some suggestions for the countermeasures.

REFERENCES

- Gu, X.Y., S.I.Tsien, H.C.Huang & Y.Liu, 1991. Analysis of Shanghai land subsidence. *Proc. 4th ISOLS*: 603-612. Houston: IAHS Publ. No.200.
- Gu, X.Y., D.N.Xu & W.Deng, 1995. A computing model based on cyclic consolidation tests. *Proc. 5th ISOLS*: 295-303. The Hague: IAHS Publ. No.234.
- Tsien, S.I. & X.Y.Gu, 1981. Computation of land subsidence in Shanghai, China. *Proc. 10th ICSMFE*, 1: 251-254. Stockholm: Balkema.